

## ARGON ION ACTIVATED DEPOSITION OF SiO<sub>2</sub> FILMS\*

S. Kitova\*, S. Youroukov, Tz. Babeva, V. Denishev, G. Danev

Central Laboratory of Photoprocesses "Acad. J. Malinowski", BAS,  
Acad. G. Bonchev str., bl.109, Sofia 1113, Bulgaria

In this paper we report our first results on the influence of the energy and current density of Ar ions in the background atmosphere on the properties of e-beam evaporated SiO<sub>2</sub> films, which are not directly bombarded by the energetic ions. Ar ions are obtained with electron cyclotron resonance source (ECR). The change of optical constants, free volume, environmental stability and adhesion of the films to the different substrates are followed.

(Received August 24, 2005; accepted September 22, 2005)

*Keywords:* SiO<sub>2</sub> films, ECR ion beam processing, Optical properties, Environmental stability, Adhesion

### 1. Introduction

Silicon dioxide is a material which is extensively used in optical thin films as protective and antireflective coating due to its low refractive index and ease of deposition. It is well known that the physical and chemical properties of films produced by physical vapour deposition deviate from these of the bulk materials and depend strongly on their microstructure [1]. Ion bombardment of the films during their deposition is a technique for improving the film properties including morphology, stoichiometry, impurity content, stress, adhesion, packing density, environmental stability, etc [2-4]. As a rule, ion bombardment of the growing film results in more compact film microstructure, without voids and cavities [3-5]. A particular advantage is the deposition of durable coatings without addition of thermal energy [3, 6]. This opens a number of applications of optical coatings on temperature-sensitive substrates.

Efficient ion bombardment is accomplished by ion of inert gases, most frequently argon. The gas introduction into the evaporation chamber, however, reduces the total pressure and the inert gas is inevitably buried in the growing film, which may change its microstructure and hence some film properties. In the case of ion assisted deposition, however, in the background atmosphere there are energetic argon ions instead of inert gas.

In this paper we report our first results on the influence of the energy and current density of Ar ions in the background atmosphere on the properties of e-beam evaporated SiO<sub>2</sub> films, which are not directly bombarded by the energetic ions. The change of optical constants, free volume, environmental stability and adhesion of the films to the different substrates are followed.

### 2. Experimental

#### 2.1. Experimental setup

Fig. 1 is a schematic diagram of the experimental set-up. High vacuum coating equipment of the type Varian 3119 with crio pump was used for conventional electron beam evaporation of

---

\* paper presented at 3<sup>rd</sup> International Symposium on irradiation phenomena in chalcogenide, oxide and organic thin films, Tryavna, Bulgaria, June 15-19, 2005.

\* Corresponding author's e-mail: skitova@clf.bas.bg

SiO<sub>2</sub> films. The vacuum system and the evaporation processes were controlled by a microprocessor-based process control unit. The SiO<sub>2</sub> source material was synthetic quartz pellets. The acceleration voltage was 10 keV and the sweep frequency was kept at 10 Hz. By varying the e-beam current a deposition rate of 6 nm s<sup>-1</sup> was achieved. The rate and the thickness of SiO<sub>2</sub> films were controlled by an Inficon IC 6000 crystal monitoring system.

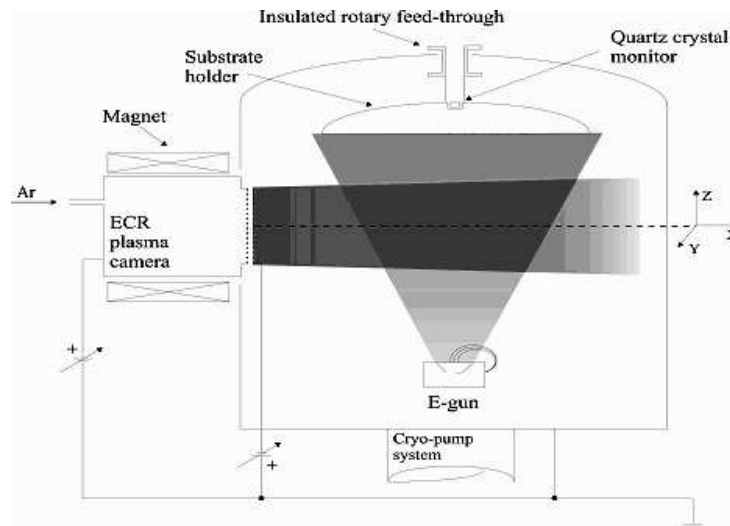


Fig. 1. A schematic diagram of the experimental set-up

Additional ECR plasma deposition apparatus was attached to the vacuum chamber. Microwave power (up to 1000 W, frequency of 2.45GHz,) is introduced into the plasma chamber through a rectangular waveguide and a window made of synthetic quartz plate. The plasma chamber operates as a microwave cavity resonator (TE<sub>11</sub> mode). Magnet coils are arranged around the periphery of the chamber for ECR plasma excitation. The circular motion frequency, electron cyclotron frequency, is controlled by the magnetic coils so as to coincide with the microwave frequency (magnetic flux density, 875G). The ECR condition enables the plasma to effectively absorb the microwave energy. Thus highly activated plasma is easily obtained at low gas pressures. The plasma source was supplied with Ar gas, controlled by a mass flow controller to generate plasma required. The Ar gas was introduced through inlet system into the plasma chamber.

Two graphite grids one called the screen grid and the other accelerator grid were used to extract ions. The distance between grids is 2mm. The total voltage applied between the grids, together with the geometrical dimensions defines the ion parameters of the source. The electric field between the grids extracts ions from the plasma through the plasma grid holes formed into small beamlets. These ions further accelerated in the gap between the grids, escape the ion source as a composite beam. This design allows extracting relatively broad ion beam of 10 cm in diameter. All measurements of ion current density were carried out by a Faraday cup.

In order to compare the influence of the energy and current density of Ar ions in the background atmosphere on the microstructure and properties of the e-beam evaporated films we chose SiO<sub>2</sub> single-layer coatings with thickness of about 150 nm for direct comparison. In each deposition various substrates were used: silicon wafers for measuring optical constants and film thickness; 80 nm thick Al film coated on glass plates and optical grade polycarbonate (PC) plates for measuring environmental stability and adhesion. All samples of PC and glass substrates were carefully cleaned. The cleaning procedure first involved washing with a 1% detergent solution and then with deionised water in an ultrasonic cleaner. A special cleaning procedure is applied for the surface of Si-wafers [7].

## 2.2. Film characterization

The refractive index  $n$  and extinction coefficient  $k$  of the films were evaluated from the reflectance of the films. The specular reflectance of the samples was measured at normal light incidence in the spectral range  $\lambda=200-1000$  nm by a Cary 5E spectrophotometer with an accuracy of

0.5%. The dispersion of refractive index  $n$  and absorption coefficient  $\alpha$  were described by the Wemple–DiDomenico single-oscillator model [8] and exponential form, respectively:

$$\varepsilon(E) = n^2(E) = 1 + \frac{E_0 E_d}{E_0^2 - E^2} \quad (1)$$

$$\alpha(E) = (4\pi kE / hc) = \alpha_0 \exp(E/A) \quad (2)$$

where  $E_d$  and  $E_0$  are the dispersion and single-oscillator energies, respectively,  $\alpha_0$  and  $A$  are constants,  $E$  – the photon energy,  $h$  is Planck constant and  $c$  is light velocity in vacuum. The initial estimates for  $E_d$  and  $E_0$  were taken from the literature [8], while these for  $\alpha_0$  and  $A$  – from a fit of the dependence of  $\alpha$  on  $\lambda$  obtained by single wavelength method TR<sub>b</sub>R<sub>m</sub> described in [9]. All initial values of model parameters, as well as the thickness were varied until a good fit between the measured and calculated values of  $R$  was found (an accuracy better than 0.5 %).

The free volume fraction  $f_b$  of the film was estimate by Maxwell Garnett effective medium expression [10]:

$$\frac{\varepsilon - \varepsilon_a}{\varepsilon + 2\varepsilon_a} = f_b \frac{\varepsilon_b - \varepsilon_a}{\varepsilon_b + 2\varepsilon_a} \quad (3)$$

where  $\varepsilon$ ,  $\varepsilon_a$  and  $\varepsilon_b$  are the dielectric functions of the films, bulk material and air ( $\varepsilon_b=1$ ) respectively at  $\lambda = 700$  nm. This expression is preferable when the volume fraction of the one of the phases is significantly lower than that of the other phase [10]. In order to determine the volume of the entrapped gas in the films obtained at  $P = 4 \times 10^{-4}$  mbar we used in our calculations for  $\varepsilon_a$ , the value of the dielectric function of the film obtained without Ar gas at  $P = 1 \times 10^{-5}$  mbar instead that of the bulk material.

To evaluate the environmental protection of the films we adopted an accelerated corrosion test [11]. Al coating, 80 nm thick, with 150 nm thick SiO<sub>2</sub> film on it were immersed into a 0.2 M solution of NaOH for 2 min. The transmission  $T$  at 633 nm after that was measured as it became more transparent upon dissolving of the Al film in the case of imperfect protection.

Adhesion of films on substrates was evaluated by cutting an “X” mark on the films with angle of 30° [12]. An adhesive tape (3M Scotch Magic Type 810) was carefully adhered to the surface of the film on room temperature. After adhesion for 1 min, the tape was pulled off rapidly back upon itself at about an angle of 180°. The peeling of the film at the X-cut area was then observed by optical microscope. Adhesion scale according to ASTM D3359-97 is following [12]: 5A – no peeling or removal occurs at all; 4A – trace peeling or removal along incisions; 3A – jagged removal along incisions occurs up to 1.6 mm; 2A – jagged removal along incisions occurs up to 3.2 mm; 1A – most of the area of the X under the tape is removed; 0A – removal of the film beyond the area of X occurs.

### 3. Results and discussion

#### 3.1. Ion beam current and profile

The ion current characteristics depend only on the total voltage, applied between the grids and are nearly independent if this voltage is achieved by the screen or accelerator voltage settings, respectively [3]. Fig. 2 shows the ion current density as a function of grid voltage at indicated Ar flow rates. The current is measured at the distance of 28 cm apart from the ion source, just above the e-gun. It is seen an increase in the ion current with an increase in grids voltage and gas flow rates. Together with initial condition at the grids, the position, the distance to the substrates and an additional processing in the beam define how the beam profile is projected into the substrate plane. The space charge in the beam may affect the resulting beam profile. The positive space charge in the beam generates a radial electrical field, which causes a radial acceleration and an additional spread of the beam.

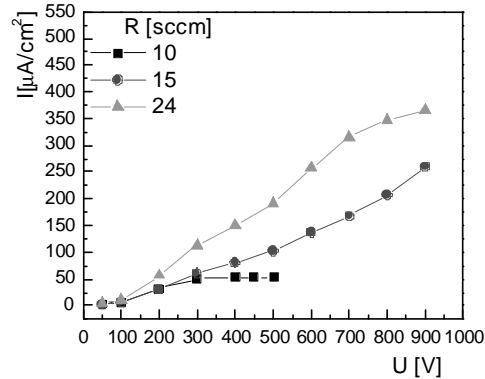


Fig. 2. Ion beam current density in dependence of grids voltage at indicated Ar flow rates. Parameters: microwave power 350 W;  $P = 4 \times 10^{-4}$  mbar. Ion beam current is measured above the e-gun at  $X = 28$  cm,  $Y, Z = 0$  cm (Fig. 1).

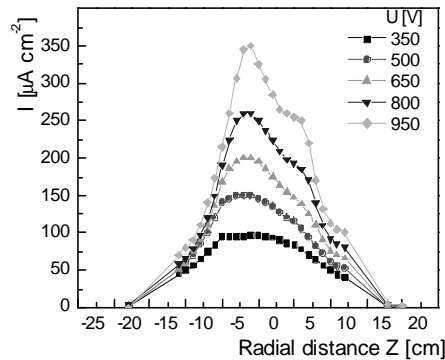


Fig. 3. Radial current density profile of Ar beam measured above e-gun ( $X = 28$  cm,  $Y = 0$  cm) at indicated grids voltages. Parameters: microwave power 350 W; Ar flow rate 15 sccm;  $P = 4 \times 10^{-4}$  mbar.

Fig. 3 shows the radial current density profile of argon ion beam apart from the ion source, obtained at different grid voltages. From the Fig. 3 it is seen that in our case (Fig. 1) the ion beam does not reach practically the substrates which are located of about 24 cm above the ion beam centre in a rotating holder, insulated from ground potential. At the same time the collisions of the initial ion beam with the evaporated particles are probable which can eventually results in one more energetic deposition as in case of sputtered deposition. In the next paragraphs we report our first results on the influence of the ion density and energy on the properties of the films obtained.

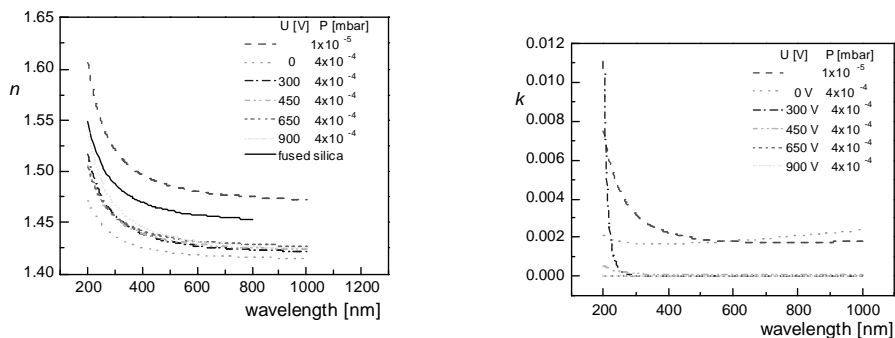


Fig. 4. Spectral dispersion of the refractive index  $n$  and the extinction coefficient  $k$  of 150 nm thick  $\text{SiO}_2$  films obtained at the indicated deposition parameters: without Ar gas at  $P = 1 \times 10^{-5}$  mbar, Ar gas, and Ar ions with different energy and current densities, extracted at indicated grid voltages  $y$  at  $P = 4 \times 10^{-4}$  mbar. Deposition rate of  $\text{SiO}_2 = 6 \text{ nm s}^{-1}$ .

### 3.2. Optical constants and free volume of SiO<sub>2</sub> films

The optical properties of films as refractive index  $n$  and extinction coefficient  $k$  depend strongly upon the film microstructure. Fig.4 shows the spectral dispersion of  $n$  and  $k$  of 150 nm thick SiO<sub>2</sub> films obtained in the presence of Ar ions with different energy and density in vacuum chamber. For comparison the refractive index of fused bulk silica [13] and that of the film deposited without Ar atoms or ions in ambient atmosphere are also given. As seen film deposited without Ar gas at  $P = 1 \times 10^{-5}$  mbar have higher refractive index than that of the stoichiometric bulk material which is indication for the oxygen deficiency in the film [14]. The introduction of Ar gas or Ar ions in vacuum chamber leads to the decrease in the film refraction index. Our calculations show that the presence of Ar gas leads to an increase of 12 % in free film volume, while in the case of energetic ion free volume increase is about 10 %, almost independently from the ion density and energy. The entrapment of gas in the films obtained at  $P = 4 \times 10^{-4}$  mbar is further confirmed from the reducing of extinction coefficient  $k$ .

### 3.3.Environmental stability and adhesion of the films

The results from the accelerated environmental test are shown in Fig. 5. It should be noted that immersion of unprotected Al film in 0.2 M NaOH leads to its complete dissolution for 1-2 min. In the case of protected with silicon dioxide Al coating the solution can get to the Al only through gap formed at points. The optical microscopy study shows that the increase in T obtained is due to the individual pinholes etched into the Al coating at defect sites in the protective SiO<sub>2</sub> film. From Fig. 5 is seen that the increase in grid voltage leads to more corrosion resistant films. As already mentioned the change of grid voltage alters simultaneously the energy and ion current density. The more detailed study shows that the improvement of film stability is mainly due to the increased ion density.

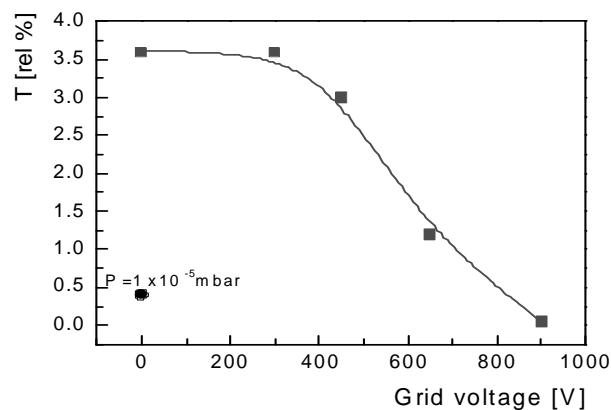


Fig. 5. Transmission of 150 nm thick SiO<sub>2</sub> films deposited on Al coated glass plates after immersion in 0.2 M NaOH for 2 min vs grid voltage.  $T_{\text{untreated sample}} = 0$ ; T of treated sample, obtained at  $P = 1 \times 10^{-5}$  mbar is indicated with fill circle.

Table 1 shows the results from the adhesion test. It is seen that the presence of energetic ion in ambient atmosphere leads to the improvement of the film adhesion to Al coatings and polycarbonate plates. Most probably the enhanced adhesion as well as the film stability are due to the enhanced mean kinetic energy of the evaporated particles as a result of the collisions with energetic Ar ions or/and of the separation of the less energetic evaporated particles under the impact of ion flux.

Table 1. Adhesion of SiO<sub>2</sub> films on Al coated glasses and PC plates in dependence of grid voltage.

Grid voltage [V] P=4 × 10 <sup>-4</sup> mbar	Adhesion	
	Al	PC
0	2A*	4A*
300	2A	4A
450	5A	5A
650	5A	5A
900	5A	5A

\* The same adhesion of films, obtained at P<sub>tot</sub> = 1 × 10<sup>-5</sup> mbar.

#### 4. Conclusion

The results obtained show that the increase in the energy and current density of Ar ions in the background atmosphere leads to the improvement of the environmental stability and adhesion of the e-beam deposited SiO<sub>2</sub> films. The more detailed study proves that these effects are mainly a result of the increased ion density. At the same time the gas volume buried in the film is almost independent of ion energy or density.

#### Acknowledgments

The authors would like to thank Prof. G. Schmahl, Dr. J. Thieme and Dr. B. Niemann from Roentgenphysik-Uni of Goettingen-Germany for their scientific support and the gift of the high vacuum coating equipment Varian 3119 and the electron cyclotron resonance ion source.

The support to this work by the Bulgarian National Science Fund (contract № Ф-1208) is gratefully acknowledged.

#### References

- [1] S. Mohan, M. G. Krishna, *Vacuum* **46**, 645 (1995).
- [2] P. Martin, *J. Mater. Sci.* **21**, 1 (1986).
- [3] J. Cuomo, S. Rosnagel, H. Kaufman, eds. *Handbook of Ion Beam Processing Technology*. Noyes Publications, ch. 1, 3 1989
- [4] G. Hubler et al, *Nuclear Instruments in Physics Research* **B46**, 384 (1990).
- [5] K. Guenter et al, *J. Vac. Sci. Technol.* **A7**, 1436 (1989).
- [6] H. Niederwald, *Thin Solid Films* **377-378**, 21 (2000).
- [7] T. Yasuda, D. E. Aspnes, *Appl. Opt.* **33**, 7435 (1994).
- [8] S. Wemple, M. DiDomenico, *Phys. Rev.* **B3**, 1338 (1971).
- [9] V. Panayotov, I. Konstantinov, *Proc. SPIE* **2253**, 1070 (1994).
- [10] D. Aspnes, *Thin Solid Films* **89**, 249 (1982).
- [11] W. Sainty, R. Netterfield, P. Martin, *Appl. Opt.* **23**, 1116 (1984).
- [12] *Standart Methods for Measuring Adhesion by Tape Test*, ASTM Designation D 3359-83 668.
- [13] H. R. Philipp, in *Handbook of Optical Constants of Solids*, E. Palik, ed. Academic Press, Inc. p. 749, 1985.
- [14] S. Durrani, M. Al\_Kuhaili, E. Khawaja, *J. Phys. Condens. Matter* **15**, 8135 (2003).